



CFD TECHNIQUES APPLIED TO AXIAL FANS DESIGN OF ELECTRIC MOTORS

Samuel Santos BORGES

*WEG, Research and Technological Innovation Department,
Rua Venâncio da Silva Porto, 399. CEP 89252-230
Jaraguá do Sul / SC - Brazil*

ABSTRACT

The objective of this work consists in presenting some characteristics of axial fans used in electric motors. The approach comprises applications, assembling, typical curves, CFD validation, design and troubleshooting of axial fans used in electric motors.

INTRODUCTION

Electric motors are widely used by humans to convert electric energy into mechanical energy. This converting process is characterized by generating losses, which are transformed into heat. To ensure the quality, safety, performance and/or efficiency of the motor this generated heat must be removed, therefore, most of the motors comprise air cooling systems. Among the components of the cooling systems, the fans are paramount. The fans can be used externally, internally or both in an electric motor, these configurations depend on the motor characteristics and its applications.

A correct fan design is very important for the temperature, losses and noise of the motor to be kept below the limits imposed by standards and/or customers. Therefore, the engineer or designer must apply the concepts of turbomachines and electric machines to properly design cooling systems.

The fans can be comprised of axial or radial rotors. In this approach, the axial rotors will be focused. Advantages and disadvantages, design fan concepts, design using computational fluid dynamics (CFD) and cases studies, are presented.

APPLICATIONS AND ASSEMBLING

The great majority of the electric motors uses radial fan with radial blades for its self ventilation. The main advantage of the radial fan is double direction of rotation. However in specific cases the electric motors comprise axial fans. This kind of fan is used for two main reasons: low noise and low absorbed power. A limitation of axial fans is single direction of rotation.

The fans are used in cooling systems of electric motors to carry the generated heat. Among many possible configurations and assembling of cooling systems, some axial fans configurations are presented next.

Internal cooling systems can be open or closed. Open drip proof motors (ODP) comprise open cooling circuit and totally enclosed fan cooled motors (TEFC) comprise closed cooling circuit. Figure 1 shows ODP and Figure 2 shows TEFC air circuits, note that OPD axial fans can be driven by the very motor shaft or by an independent one.

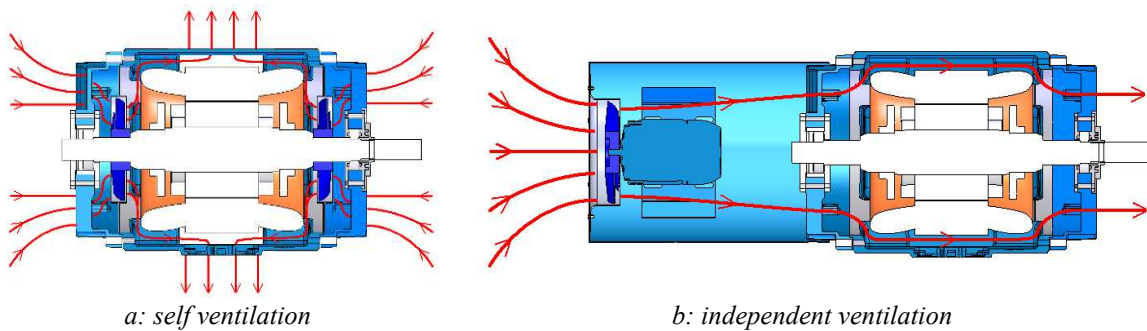


Figure 1: ODP motor scheme

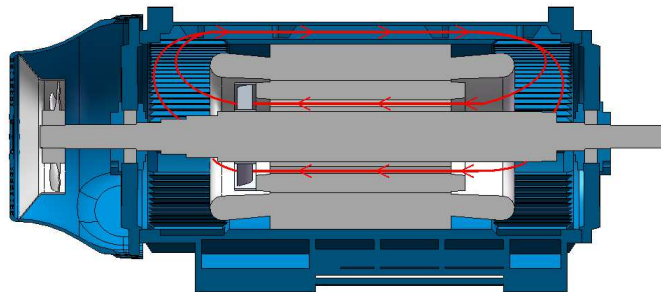


Figure 2: TEFC motor scheme with self internal ventilation

External cooling systems are mostly used in TEFC motors and can be driven by the very motor shaft or by an independent one; two examples are presented in Figure 3.

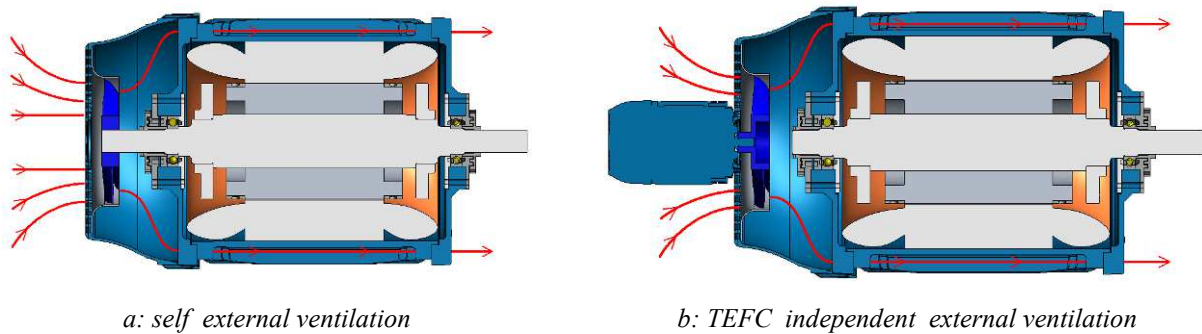
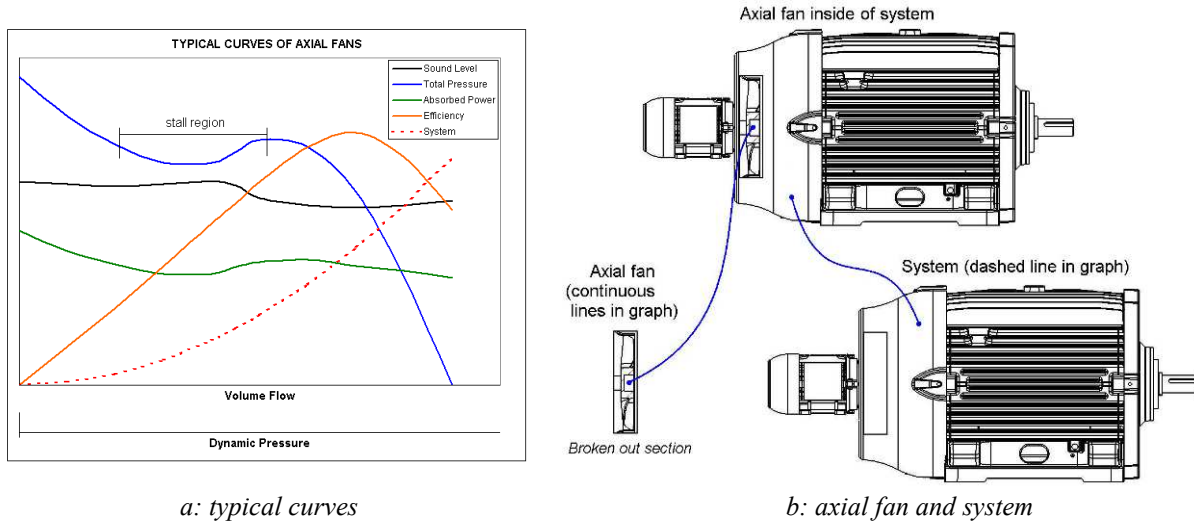


Figure 3: TEFC motor scheme

TYPICAL CURVES

The typical performance of an axial fan is represented by curves of volume flow, dynamic pressure, total pressure, absorbed power, efficiency and noise, as shown in Figure 4a. In the region before maximum efficiency occurs the stall effect, which causes a noise increase and aerodynamic instability therefore the avoidance of this region is desirable in fan design.

The curves in graph are related to Figure 4b, which presents a TEFC scheme; all the continuous lines are axial fan characteristics and the dashed line is a motor characteristic.



a: typical curves

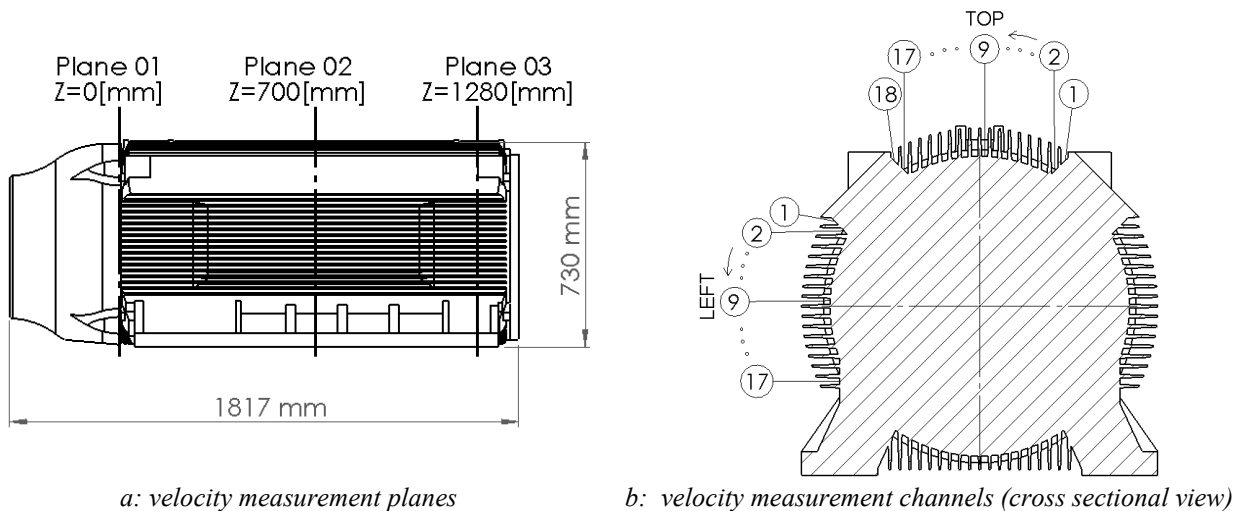
b: axial fan and system

Figure 4: typical curves of axial fan and system

CFD VALIDATION

CFD is a powerful tool for cooling systems design of electric motors, mainly by the complex characteristics of geometries and air flows involved in such applications. However, for the CFD results to be safe and reliable with any design, the validation process is fundamental. Therefore, this section concerns the validation of CFD to be used in axial fan design.

The first comparison includes the air velocity validation. In this stage, 400 kW motor was used; the measurement points are identified in Figure 5a by planes and in Figure 5b by channels number.



a: velocity measurement planes

b: velocity measurement channels (cross sectional view)

Figure 5: velocity measurement positions

Taking the back view as reference, the measurement points are located on the top and on the left side of the motor. The terminal box is attached on the right side of the motor, as shows the Figure 6a, therefore the air velocities were not measured in this side.

Figure 6b presents a Pitot tube in the center of the channel; all the air velocities were measured as shown in the figure.



a: right view of motor



b: air velocity measurement (dynamic pressure) with Pitot tube

Figure 6: motor and measurement probe

After experimental data acquisition the CFD analysis was made to compare between experimental with simulated data. Therefore the main simulation data are included in Table 1; furthermore it is important to mention the boundary conditions. For each simulation, two domains are created: one rotating and other stationary for the fan rotor and the motor, respectively, which are connected by fluid-fluid interfaces. The rotating domain is bounded by interfaces, rotor and volute external surfaces. And the stationary domain is bounded by interfaces, motor external surfaces and far field surface. Far field surface is located far away from the motor and its relative pressure is 0 Pa.

Table 1: CFD simulation data

| | |
|-----------------------------|------------------------------|
| CFD software: | Ansys CFX – version 13.0 |
| Nodes number: | 4,921,883 |
| Analysis type: | steady state |
| Heat transfer model: | isothermal |
| Fluid: | Air at 25 °C |
| Turbulence model: | Shear stress transport (SST) |
| Maximum residual: | 2.4E-05 rms |
| Iteration number: | 1000 |

The important parameter to CFD is the space domain discretization, called mesh. A technique used to check the reliability of mesh consists in the mesh refinement and for each mesh generated a simulation is accomplished. In these simulations some points of concern are monitored, in this case six velocity points have been monitored and the results are presented in Figure 7. The curves show stabilization of results from 5,000,000 nodes, what indicates a good mesh refinement. The refinements have been carried out in regions of concern and large residuals.

The simulated geometry mesh (Figure 8a) shows that the region of the top channels requires more refinement because it is a measurement region. Figure 8b presents the air flow streamlines over the motor.

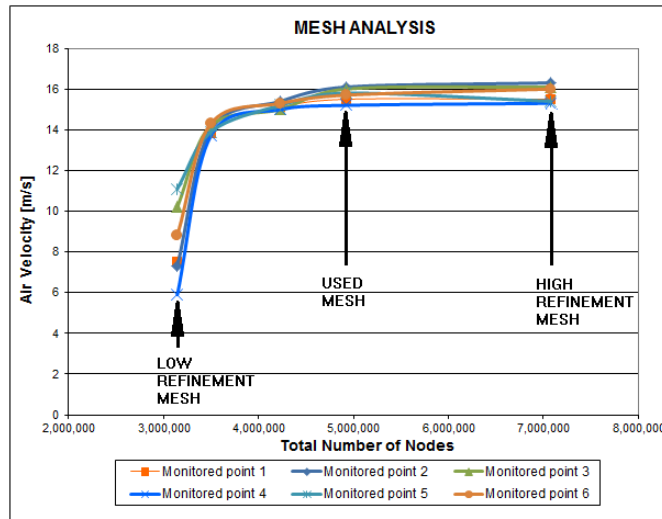
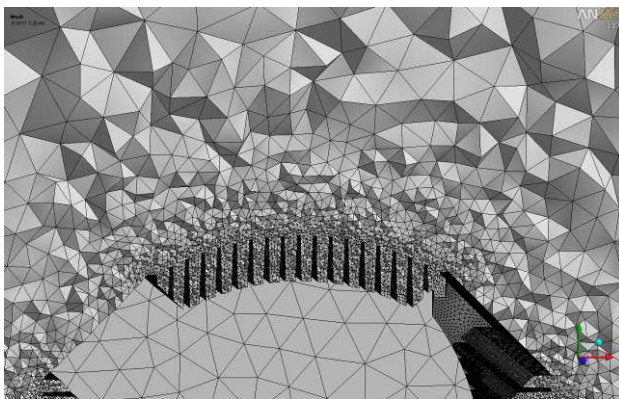
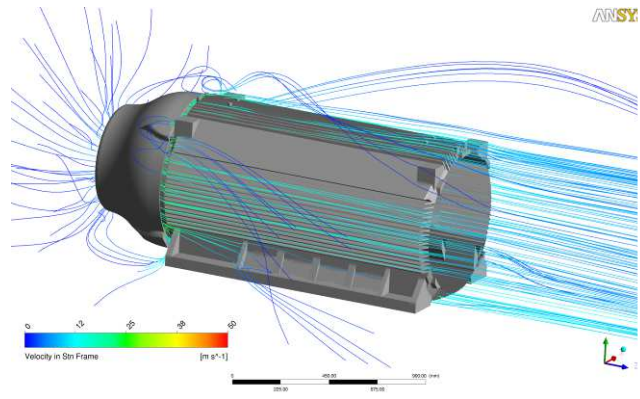


Figure 7: mesh analysis



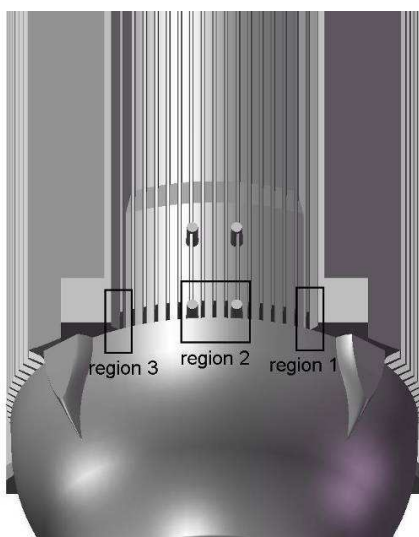
a: channels mesh



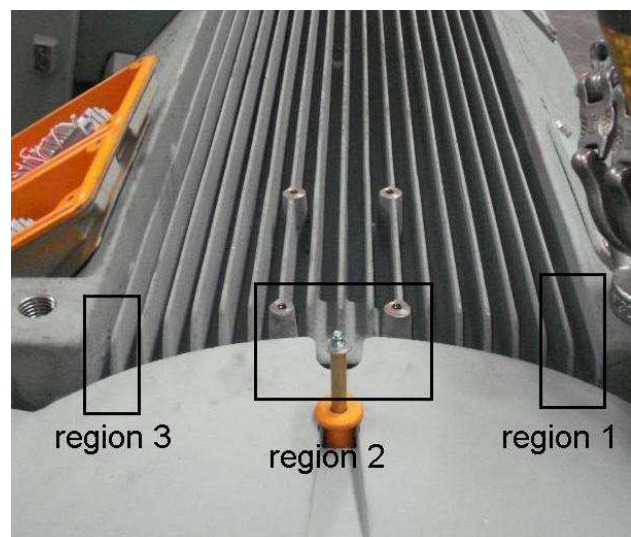
b: air flow streamlines

Figure 8: mesh and streamlines on motor

Some differences between the simulated and the measured geometry occurred due to the adjustment requirements of the tested motor. The region 2 in the Figure 9 is the most critical one on the top, because it contains geometric difference on the fan cover and frame motor. Regions 1 and 3 contain only differences in the frame channels.



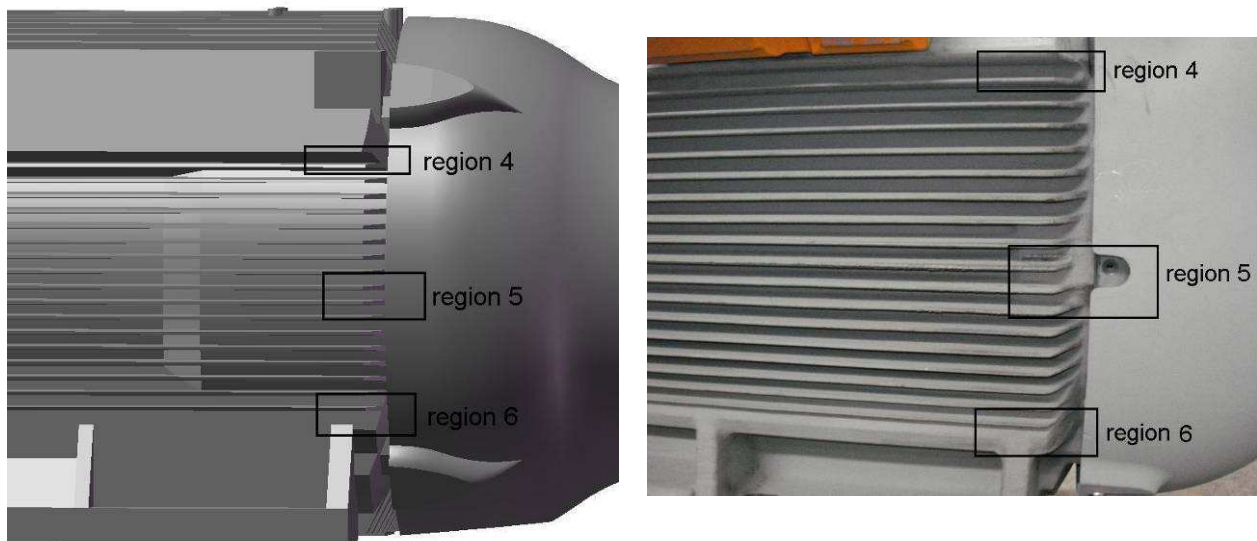
a: simulated geometry (top view)



b: tested geometry

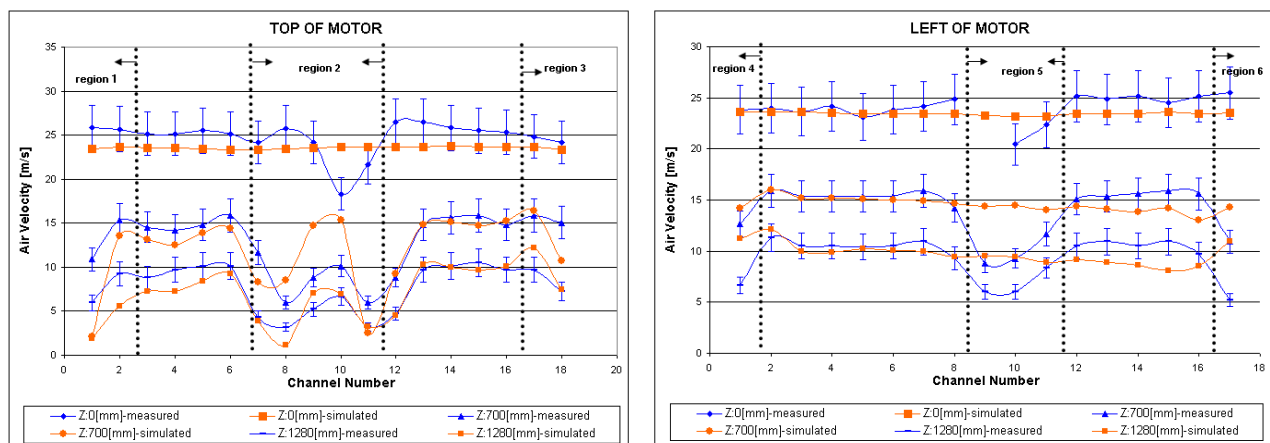
Figure 9: simulated and tested geometry on the top of motor

Similarly, the region 5 is the most critical one on the frame side; once that it contains differences both in the fan cover and in the frame, whereas in regions 4 and 6 geometric differences between the simulated and the actual models exist only in the frame channels. These regions are identified in Figure 10.



a: Simulated geometry (left view) b: tested geometry
 Figure 10: simulated and tested geometry on the left side of motor

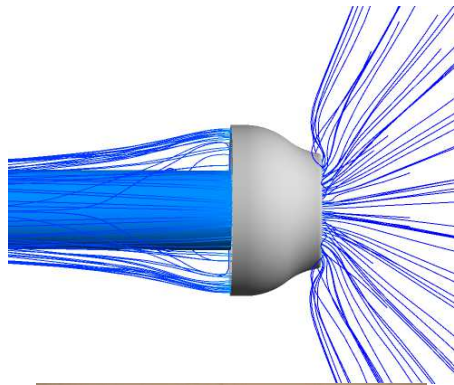
The comparison results are presented next. Figure 11a shows the air velocity on the motor top and Figure 11b shows the air velocity on the motor left side. Note that in the regions outside the critical ones the results are satisfactory in the most measured point. The plane 01 measurements contain more errors because the Pitot tube was positioned outside the channels; specifically in this case the measurements were realized between channels and fan cover. In these figures the blue and the orange lines correspond to simulation and measurement results, respectively. Note: the channel 9 – plane 1 – left side was not measured.



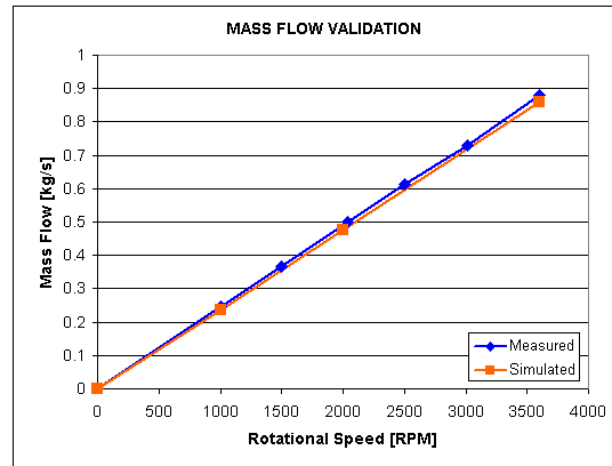
a: air velocity on top of motor b: air velocity on left side of motor
 Figure 11: simulation and measurement comparison

The second validation is related to mass flow and not used the same motor of the previous validation. For this analysis, a simplified device (Figure 12a) was made with the end shield, fan cover, volute and rotor fan to adjust the ventilation system in the test bench.

For this analysis, the criteria and CFD data (Table 1) of simulation were the same of previous simulation. The main differences are the node numbers: 225,241, maximum residual: 3.5E-05 rms and iteration number: 1715. The results are shown in Figure 12b, where the simulated and measurement values are very closed; the maximum error presented was 2.6 %.



a: simplified ventilation systems



| RPM | Mass Flow [kg/s] | | |
|------|------------------|-----------|-----------|
| | Measured | Simulated | Error [%] |
| 0 | 0 | 0 | 0 |
| 1000 | 0.244 | 0.238 | -2.5 |
| 2000 | 0.488 | 0.475 | -2.6 |
| 3600 | 0.879 | 0.861 | -2.0 |

b: mass flow results

Figure 12: mass flow in simplified device

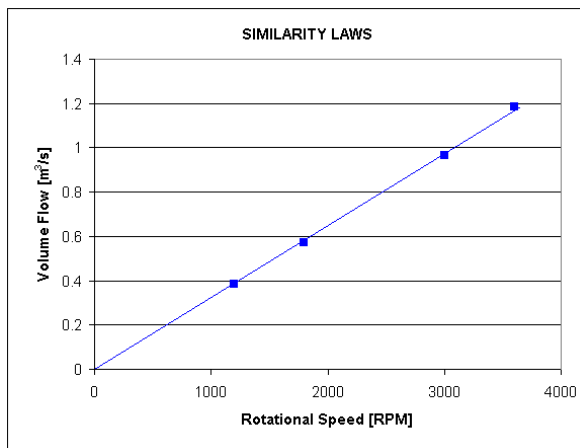
SIMILARITY LAWS USING CFD

The application of similarity laws in fans design is an important methodology to decrease design time, estimate performance outside the tested condition and among other reasons. The aim of this section is to present some proposals to extend these laws to others variables applied in motor cooling systems.

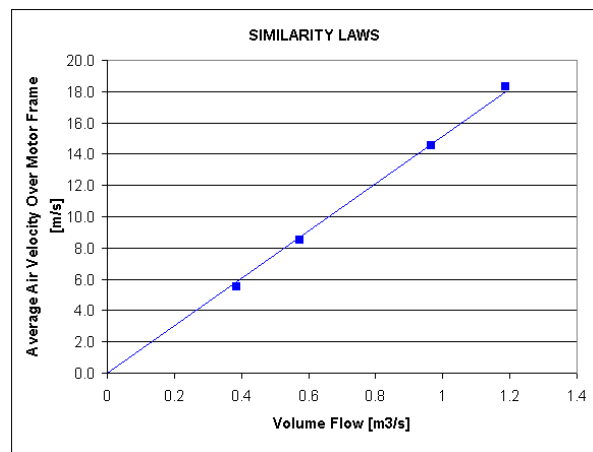
Temperature field is an important parameter that must be calculated in motor design; therefore the heat transfer coefficient, an air velocity-dependent variable, is required.

Currently, the electric motors often use frequency converter to operate in several rotation speeds, then relating the rotation speed to the air velocity over the motor is an easy way to estimate the temperature in several rotation speeds. Temperature can be predicted as proposed in [2]

The computational simulation results presented in Figure 13a relate rotation speed to volume flow, a known similarity law. Figure 13b shows the interrelation between volume flow and average air velocity over motor frame.



a: rotational speed x volume flow



b: volume flow x average air velocity

Figure 13: similarity laws

The volume flow varies linearly with both the rotational speed and the air velocity, thus

$$\frac{RPM_1}{RPM_2} = \frac{\dot{V}_1}{\dot{V}_2} = \frac{Vel_1}{Vel_2} \quad (1)$$

Where,

RPM : rotation speed;

\dot{V} : volume flow;

Vel : average air velocity over motor frame;

1: known variable;

2: unknown variable.

The equation (2) is a geometric similarity law modification that purposes volume flow estimative from fan rotors relationship. This approach can be used in cases where only fan rotors and volutes are changed.

$$\frac{\dot{V}_1}{\dot{V}_2} = \left(\frac{\phi_{rot1}}{\phi_{rot2}} \right)^{3 * \left(\frac{\phi_{rot1} + \phi_{rot2}}{2 * \phi^{cov}} \right)} \quad (2)$$

Where,

\dot{V} : volume flow;

ϕ_{rot} : rotor fan diameter;

ϕ^{cov} : fan cover diameter;

1: known variable.

2: unknown variable.

Table 2 presents a comparison between simulation and analytical estimation values, note that accuracy is around of 10 %. Therefore, this equation can be used only as an approximation.

Table 2: Simulation and estimated data

| Condition | CFD Simulation | | Estimated by (2) | | Error [%] |
|-----------|---------------------------|--|---------------------------|--|-----------|
| | $\phi_{rot}^{1)}$ [mm] | Volume Flow ¹⁾ [m ³ /s] | $\phi_{rot}^{1)}$ [mm] | Volume Flow ²⁾ [m ³ /s] | |
| 1 | 355 | 1.187 | 400 | 1.405 | -9.8 |
| 2 | 355 | 1.187 | 500 | 2.055 | -8.5 |
| 3 | 400 | 1.558 | 500 | 2.270 | 1.1 |
| 4 | 400 | 1.558 | 355 | 1.316 | 10.9 |
| 5 | 500 | 2.246 | 355 | 1.297 | 9.3 |
| 6 | 500 | 2.246 | 400 | 1.541 | -1.1 |

¹⁾ Known variables. ²⁾ Unknown variables.

The motors components are presented in Figure 14. This scheme can be used as support for the understanding of the motor ventilation systems.

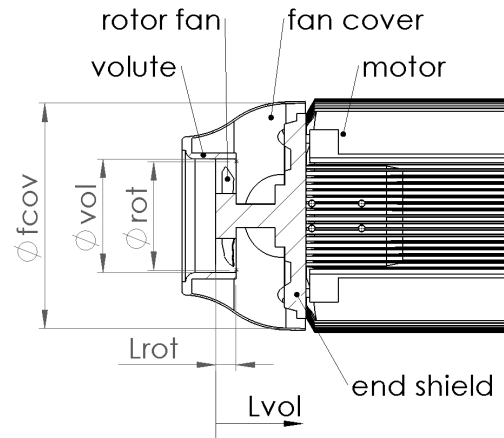


Figure 14: identification of the motor components

FAN DESIGN

The concept of fan rotor design used in electric motors is the same of that of conventional fans. However, the recommended range of angle β is from 18° to 45° and typical c_m values are 4 m/s up to 30 m/s. For the blades, many types of profiles can be used, for example the GÖ 490 and the NACA 4409. Figure 15 presents the blade components of geometry and flow.

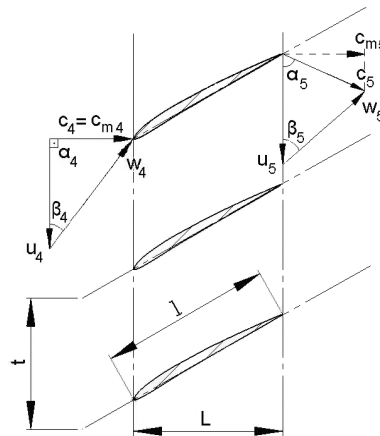
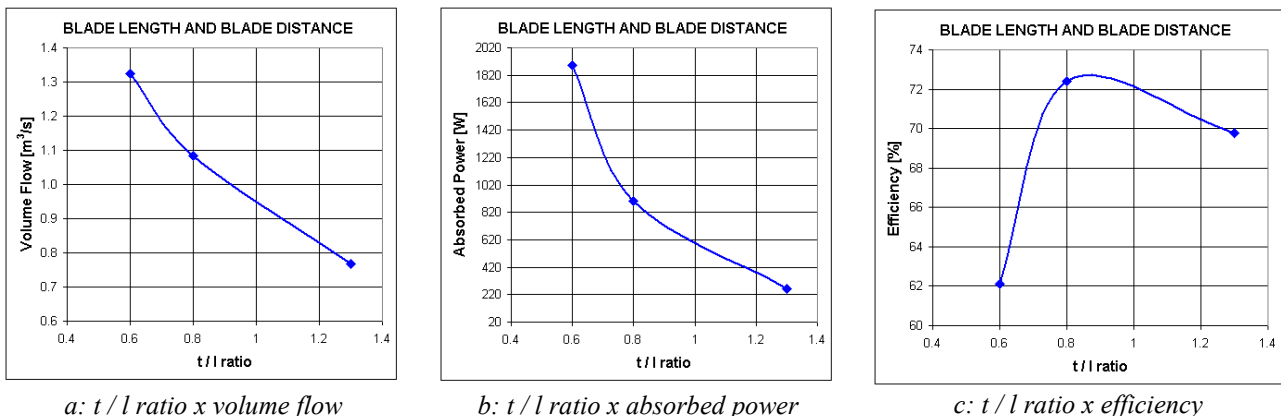


Figure 15: blade components for axial rotor

The t/l ratio has great influence in the fan performance as shown in Figure 16. Note that, the best t/l ratio for optimal efficiency purpose is between 0.8 and 0.9. The simulation results presented refer to a single rotor and the t/l ratio was kept constant along the blade diameter and it was obtained through L reduction, keeping the same angles and shape of blade from leading edge side (side of c_4) and cutting the side of trailing edge (side of c_5).



a: t/l ratio x volume flow

b: t/l ratio x absorbed power

c: t/l ratio x efficiency

Figure 16: t/l ratio effect in fan performance

The adjustment between volute and fan rotor is essential for the good performance of the ventilation system. Figure 17 presents the air velocity vectors resulting from different configurations of volutes applied to the same rotor. The rotor diameter is 355 mm and the volute diameter varies as indicated below in each simulation result. The images had been taken in a plane section that contains the rotational axis and show the blade tip; the vectors present the tangential projection of the velocity field in this plane.

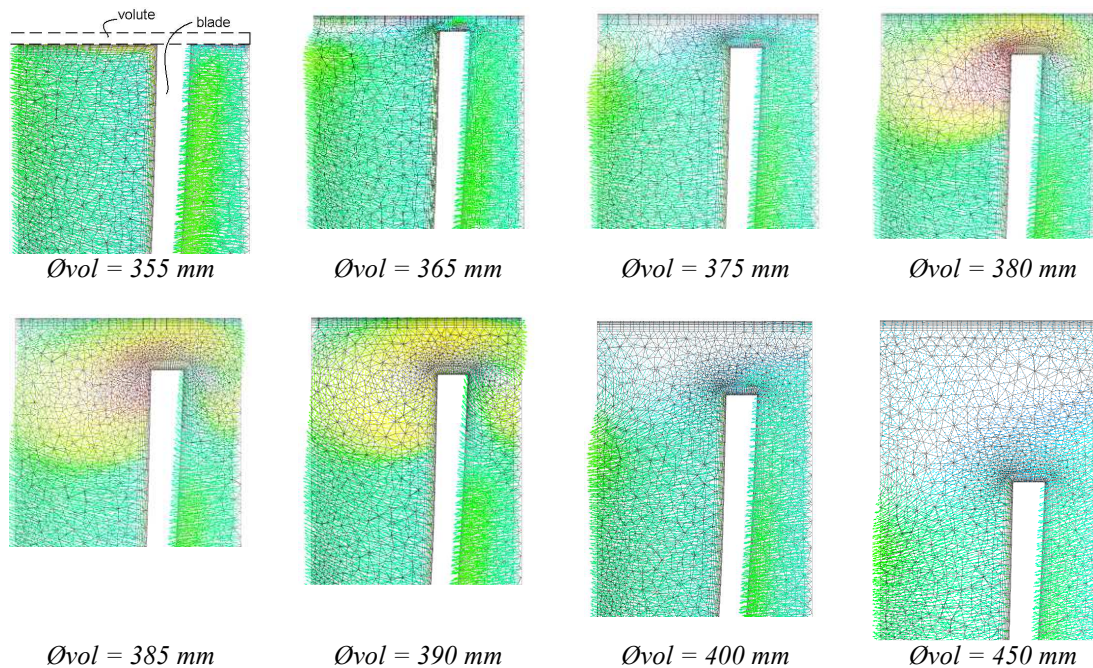


Figure 17: gap between volute and fan rotor

Figure 18 shows a transversal section views of a 0.73 blade radius. The absolute air velocity vectors in Figure 18a correspond to the best configuration according to simulation results; note that such vectors are approximately aligned with the rotation axis. In Figure 18b, which correspond to the lower efficiency configuration, the vectors are disordered.

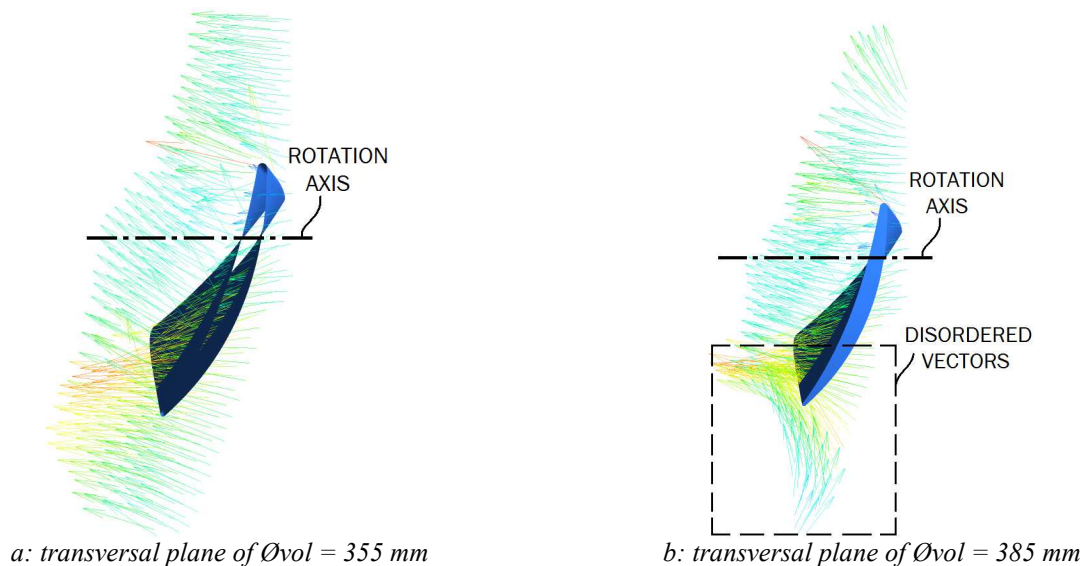
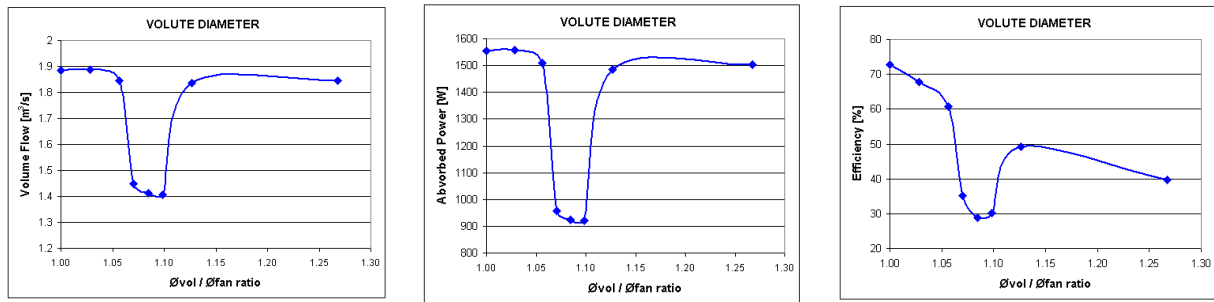


Figure 18: absolute velocity vectors in transversal section view of a 0.73 blade radius

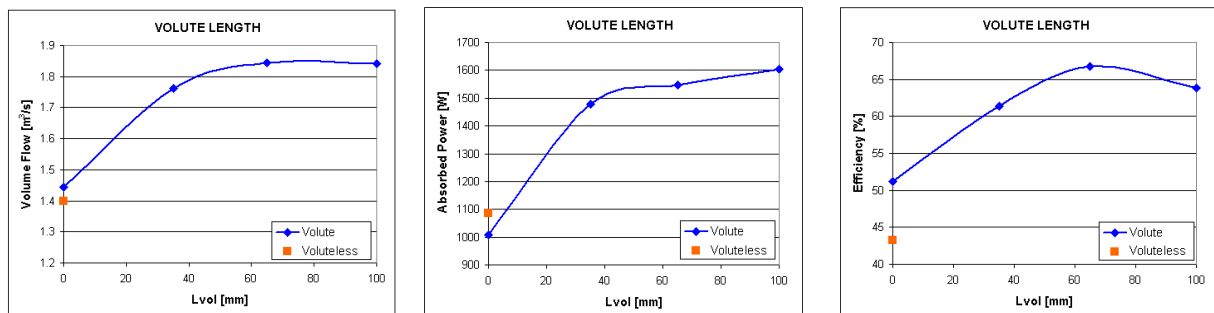
In the next figure, the volume flow, the absorbed power and the efficiency are plotted as a function of the volute diameter per the rotor fan diameter ratio. When the ratio between volute diameter and rotor fan diameter is equal to one, it is the best configuration. When this ratio is between 1.07 and 1.12 there is a performance decrease, which can mean a stall condition.



a: $\text{Øvol} / \text{Øfan ratio} \times \text{volume flow}$ b: $\text{Øvol} / \text{Øfan ratio} \times \text{absorbed power}$ c: $\text{Øvol} / \text{Øfan ratio} \times \text{efficiency}$

Figure 19: $\text{Øvol} / \text{Øfan ratio}$ effect in fan performance

Using a 365 mm volute diameter the volute length (L_{vol} in Figure 14) was evaluated. The results of this analysis are presented in the Figure 20 and the optimal length is 65 mm, the same length of the rotor. The efficiency was calculated using total pressure in a plane of the fan cover outlet.



a: $L_{vol} \times \text{volume flow}$ b: $L_{vol} \times \text{absorbed power}$ c: $L_{vol} \times \text{efficiency}$

Figure 20: volute length (L_{vol}) effect in fan performance

FANS TROUBLESHOOTING

The axial fans can present unsteady flow characterized for bad used conditions, which are known as stall, surge and instabilities. These conditions cause some problems as noise and vibration levels increase. As an example, an area restriction of 50 % between end shield and fan cover of a 315 kW motor caused an increasing in the punctual noise of 87.4 dB(A) to 94.9 dB(A), as a result of an inappropriate change in the motor working condition.

CONCLUSIONS

Axial fans must be used in electric motors in conditions where the rotation direction is defined and the pressure drop is low. The great advantages provided by this type of fan are low noise and low absorbed power. The axial fan design is complex and involves many design variables. Among various considerations that must be made, the conditions of stall, surge and instabilities must be avoided to insure a good performance.

CFD application in design of axial fans presents many advantages such as design time reduction and facilities of flow estimation and visualization. However, validation is an important stage to ensure quality and reliability of simulation results.

ACKNOWLEDGMENTS

The author would like to thank all Weg colleagues that directly or indirectly participated in this project. Mainly to Ricardo Felipe Junckes, Thiago Schwinden Leal and Waldiberto de Lima Pires.

BIBLIOGRAPHY

- [1] *ANSI/ASHRAE 51-07. Laboratory Methods of Testing Fans for Certified Aerodynamic Performance Rating.* **2007.**
- [2] C. A. Cezário, H. P. Silva – *Electric Motor Winding Temperature Prediction Using a Simple Two-Resistance Thermal Circuit.* 18th International Conference on Electrical Machines – ICEM - 2008. Vilamoura, Portugal. 6-9 September **2008.**
- [3] C. Pfleiderer, H. Petermann – *Máquinas de Fluxo.* Quarta edição. Berlin / Heidelberg. **1972.**
- [4] F. Kameier, W. Neise – *Experimental Study of Tip Clearance Losses and Noise in Axial Turbomachines and Their Reduction.* Journal of Turbomachinery. Vol. 119. July, **1997.**
- [5] F. P. Bleier – *Fan Handbook – Selection, Application and Design.* USA. **1998.**
- [6] F. R. Menter – *Two-Equation Eddy-Viscosity Turbulence Models for Engineering Applications,* AIAA Journal, vol. 32, no 8. pp. 1598-1605, **1994.**
- [7] F. R. Menter – *Zonal Two Equation k - ϵ Turbulence Models for Aerodynamic Flows,* AIAA Paper 93-2906, **1993.**
- [8] G. F. Round – *Incompressible Flow Turbomachines – Design, Selection, Applications and Theory.* USA. **2004.**
- [9] *IEC 60034-6: Rotating Electrical Machines - Part 6: Methods of Cooling (IC Code).* 2nd edition. **1991-10.**
- [10] L. Neuhaus, W. Neise – *Active Flow Control to Improve the Aerodynamic and Acoustic Performance of Axial Turbomachines.* 1st Flow Control Conference. 24 – 27. St. Louis, Missouri. June, **2002.**
- [11] R. Bran, Z. de Souza – *Máquinas de Fluxo – Turbinas, Bombas e Ventiladores.* Rio de Janeiro. **1969.**
- [12] R. Jorgensen – *Fan Engineering.* Sixth edition. Buffalo, New York. **1961.**